Myosin Subfragment 1 Activates ATP Hydrolysis on Mg^{2+}-G-Actin†

Andrzej A. Kasprzak

Centre de Recherches de Biochimie Macromolèculaire, CNRS-INSERM U. 249, Université de Montpellier I, 34033 Montpellier, France

Received April 11, 1994; Revised Manuscript Received July 8, 1994®

ABSTRACT: The interaction of myosin subfragment 1 isoenzyme A2 (S1A2) with Mg^{2+}-G-actin was studied. Polarization titrations of 1,5-IAEDANS-Mg^{2+}-G-actin and of ϵATP-Mg^{2+}-G-actin with S1A2 provided evidence that, similar to Ca^{2+}-G-actin, the proteins form a tight binary complex. Significant amounts of oligomeric forms of actin in the presence and absence of S1 were not detected. The effect of S1A2 on the rates of nucleotide and metal dissociation and hydrolysis from Mg^{2+}-actin was measured. The hydrolysis rate for [γ-^{32}P]ATP-actin in the G-acto-S1A2 complex ($k_- = 0.016$ s^{-1}) was faster than the rate of ^{32}P liberation from the complex ($k_- = 0.004$ s^{-1}), obtained by measuring the liberation of [^{32}P]orthophosphate from [α-^{32}P]ATP-actin in the presence of a large excess of alkaline phosphatase. This indicates that most of actin's ATP was hydrolyzed before it was released to solution and that the dissociating nucleotide was ADP, for which the dissociation rate is higher than that for ATP. In agreement with this mechanism, S1A2 accelerated the dissociation of ϵATP but inhibited the dissociation of ϵADP from the complex. The activation of actin's ATPase is specific for Mg^{2+}-G-actin and does not occur in Ca^{2+}-G-actin. The effect of deoxyribonuclease I on the rates of nucleotide dissociation and hydrolysis was examined. Although the ATPase of actin was also stimulated by S1A2 in the presence of deoxyribonuclease I, the reaction was considerably slower in this case ($k_- = 0.001$ s^{-1}), showing the importance of the motion of the two large actin domains for nucleotide exchange and hydrolysis. The significance of this finding for elucidation of the effects of S1 on the actin structure and the possible role of ATP hydrolysis by G-actin in the regulation of cytoskeleton are discussed.

Considerable progress in understanding the structure of actin has been made in the last few years. Following the resolution of the atomic structure of the actin monomer (Kabsch et al., 1990) and a preliminary reconstruction of the actin filament (Holmes et al., 1990), other laboratories solved the X-ray structure of actin in its complex with segment 1 of gelsolin (McLaughlin et al., 1993) and proposed a high-resolution structure for profilactin (Schutt et al., 1993). Recently, Lorenz et al. (1993) obtained a refined model of the actin filament that almost perfectly accounts for the X-ray fiber diffraction pattern obtained from actin gels. These advances explained a number of crucial biochemical and biophysical observations and shed more light on the evolution of the actin molecule and its structural relation to other proteins (Bork et al., 1992). They also enabled, for the first time, a reconstruction of the complex of F-actin with myosin subfragment 1 (S1[1]) (Rayment et al., 1993; Schröder et al., 1993). Nevertheless, several key structural questions still remain unanswered.

For example, the structural difference between ADP- and ATP-actin is not clear. These species are biochemically distinguishable, and thymosin β_4 (Carlier et al., 1993), actophorin (Maciver & Weeds, 1994), and presumably gelsolin (Laham et al., 1993) rely on such differences, but the structure of monomeric actin does not offer any clues about how the proteins might recognize these forms. Second, the actin used for almost all structural studies and a majority of the biochemical data had a Ca^{2+} ion at its tight-binding site. However, this is not the physiologically relevant actin form, which is believed to be Mg^{2+}-actin. In the G-form, Ca^{2+}- and Mg^{2+}-actin have a number of dissimilar properties [Orlova & Egelman, 1993; Strzelecka-Golaszewska et al., 1993; for a review see Estes et al. (1992a)]. Furthermore, the differences do not disappear upon actin polymerization. Both Harwell et al. (1980) and Orlova and Egelman (1993) observed that Mg^{2+}-F-actin filaments were more flexible than those obtained in the presence of Ca^{2+}. In many ways, this increase in the flexibility of Mg^{2+}-F-actin resembles the effect S1 exerted on the flexibility of the actin filament (Orlova & Egelman, 1993; Yanagida et al., 1984) and could explain the extensive undulation of the filament by S1 (Ménétret et al., 1991).

Recently, I used the Ca^{2+}-G-acto-S1A2 complex to elucidate the structural changes in actin induced by S1 binding (Kasprzak, 1993). The significance of such an approach, i.e., the use of G-actin, received further support from comparison of the structure of the G-actin monomer with that of the F-actin protomer. Both forms of actin exhibit extensive similarities, and the observed differences were localized in the DNase binding loop in subdomain 2. Some additional distortions in subdomain 4 were also seen (Lorenz et al., 1993). Thus, with the exception of these two regions, studies on the G-acto–S1 complex provide invaluable insights into the structural alterations in actin caused by interaction with S1. Of course, one must bear in mind that, in the filament, both the actin protomer and S1 can interact with another actin molecule(s), creating a more complex interface, but the G-acto-S1 system

† Funds for this research were provided by the Centre National de la Recherche Scientifique, the Institut National de la Santé et de la Recherche Médicale, and the Association Française contre les Myopathies.

® Abstract published in *Advance ACS Abstracts,* September 15, 1994.

[1] Abbreviations: ϵATP and ϵADP, 1,N^6-ethenoadenosine 5′-triphosphate and -diphosphate; S1, myosin subfragment 1; S1A2, isoenzyme of myosin subfragment 1 carrying alkali light chain A2; DTE, dithioerythritol; HEPES, *N*-(2-hydroxyethyl)piperazine-*N*′-2-ethanesulfonic acid; 1,5-IAEDANS, *N*-(iodoacetyl)-*N*′-(5-sulfo-1-naphthyl)ethylenediamine; EDTA, ethylenediaminetetraacetic acid; EGTA, ethylene glycol bis(β-aminoethyl ether)-*N,N,N*′,*N*′-tetraacetic acid; DNase I, deoxyribonuclease I; pPDM, *p*-phenylenedimaleimide.

0006-2960/94/0433-12456$04.50/0

is important because of its simplicity. In the present work, I extended the studies of this complex with Mg^{2+}-G-actin and explained a somewhat puzzling initial observation that for ADP-G-actin, S1 inhibits the dissociation of the nucleotide and of the magnesium ion, whereas for ATP-G-actin it accelerates their dissociation. A preliminary report of these results has appeared (Kasprzak, 1994).

MATERIALS AND METHODS

Proteins. Column-purified G-actin and S1A2, both from rabbit skeletal muscle, were prepared as described previously (Kasprzak, 1993). Commercially available DNase I (Boehringer Mannheim), purified according to Price et al. (1969), was the gift of Karine Lheureux. Mg^{2+}-actin was prepared from Ca^{2+}-actin by incubating the latter at a concentration of *ca.* 20 μM in buffer G_C (2 mM HEPES, 0.1 mM $CaCl_2$, 0.2 mM DTE, 0.1 mM NaN_3, 0.1 mM $MgCl_2$, and 0.25 mM EGTA, pH 8.0) for 10 min. The protein was used within the next 5–10 min; for example, for titration curves shown in Figures 1 and 3, a separate conversion of Ca^{2+}- to Mg^{2+}-actin was performed before each measurement. It was verified, by the increase in the fluorescence of 1,5-IAEDANS conjugated with Cys-374 of actin, that the metal exchange was complete in 1–1.5 min at 20 °C. When the ϵATP-Ca^{2+}-actin complex is incubated with EGTA/Mg^{2+}, in the absence of external nucleotide, partial dissociation of ϵATP from actin occurs. To minimize the loss of nucleotide, all conversions were done using actin at a concentration of about 20 μM; as judged from the decrease in the ϵATP fluorescence, in 10 min less than 10% of the nucleotide dissociated from actin.

Exchange of ATP by ϵATP was done as described elsewhere (Kasprzak, 1993). To replace ATP with either [γ-^{32}P]ATP or [α-^{32}P]ATP (both from Amersham), the same protocol was followed, with the exception that the ATP (5 μM) initially present in actin preparations (Kasprzak, 1993) was removed by AG 1x8 resin.

ϵADP-actin was prepared essentially as described by Pollard et al. (1992), using ϵADP (Sigma) at concentration of 0.8 mM. Both agarose-immobilized and soluble hexokinase (Sigma) were employed with similar results. While soluble hexokinase cannot be used for nucleotide *exchange* experiments, it can be used in the system with alkaline phosphatase to measure the rate of nucleotide *dissociation.* ϵADP-actin was kept on ice and used within 2 h.

Binding and Kinetic Experiments. For all binding and kinetic experiments, buffer G_M (2 mM HEPES, 0.05 mM $MgCl_2$, 0.1 mM EGTA, 0.2 mM DTE, and 0.1 mM NaN_3, pH 7.5 at 20 °C) was employed. The buffer was prepared fresh each week. In all binding experiments, the fluorescence anisotropy was measured with the polarization accessory of a Perkin-Elmer LS50 fluorometer using the conditions given for 1,5-IAEDANS-actin by Chaussepied and Kasprzak (1989a) and for ϵATP by Kasprzak (1993). For kinetic measurements, the decrease in ϵATP fluorescence was followed with a Kontron SFM 25 fluorometer. The reaction of the nucleotide dissociation was initiated by simultaneous addition of Mg^{2+}-actin, alkaline phosphatase (50 units/mL), or EDTA and eventually S1. Premixing of actin and S1 and adding alkaline phosphatase or EDTA later resulted in a lower zero-time fluorescence intensity but did not change the rate constant of the reaction. Since both Mg^{2+} and Zn^{2+} ions have to be removed from solutions of alkaline phosphatase, the enzyme undergoes partial inactivation. Consequently, the exact amount of phosphatase activity actually added was not known. It was, therefore, essential to verify each time that the amount of added enzyme was not a limiting factor in the dissociation of the actin nucleotide.

Light-scattering measurements were made using a Kontron SFM 25 fluorometer and employing excitation and emission wavelengths of 400 nm.

Radioactive [^{32}P]ATP was diluted upon arrival with cold nucleotide to a concentration of 1 μCi/μL. After the incubation of actin with either [γ-^{32}P]ATP or [α-^{32}P]ATP, the 1:1 complexes of Ca^{2+}-ATP-actin were converted to the Mg^{2+} form. At time = 0, alkaline phosphatase (*ca.* 50 units/mL), S1A2, and/or DNase I (14 μM) were added. Aliquots were withdrawn from the reaction mixture; the reaction was stopped, and the ^{32}P liberated was quantified by first converting the [^{32}P]orthophosphate to a phosphomolybdate complex with 10 mM ammonium molybdate in 1 M HCl/0.65 M $HClO_4$ and then extracting the complex with a solution of cyclohexane/isobutyl alcohol/acetone (50:50:10) saturated with ammonium molybdate solution (Valentin-Ranc et al., 1991). The radioactivity was counted in a Beckman SC 6000 liquid scintillation counter using 10 mL of liquid scintillation cocktail (Optima, Packard).

Data Analysis. The equilibrium and kinetic parameters for the data shown in this paper have been computed by fitting the experimental points to the following equations: For a fluorescence decrease during ϵATP or ϵADP dissociation, eq 1 was used:

$$F = F_\infty + (F_0 - F_\infty) \exp(-kt) \quad (1)$$

For the time course of the liberation of ^{32}P, eq 2 was employed:

$$F = F_0 + (F_{max} - F_0)[1 - \exp(-kt)] \quad (2)$$

In these equations, F and F_{max} denote the current and maximal values of the measured parameter (fluorescence intensity or fraction of ^{32}P liberated), respectively, F_0 is its value at time = 0, t is the time, and k is the dissociation rate constant. Both equations are essentially equivalent and describe first-order kinetics. The binding parameters for the interaction of S1A2 with Mg^{2+}-G-actin were obtained by a fit to eq 3:

$$\Delta A = \Delta A_{max}\{W - (W^2 - [S1]_t/(n[G]))^{1/2}\} \quad (3)$$

where $W = (K_d + [S1]_t + n[G])/(2n[G])$, ΔA denotes the value of fluorescence anisotropy obtained at total S1 concentration $[S1]_t$, ΔA_{max} is the anisotropy value at saturation, [G] is the concentration of G-actin, K_d is the dissociation constant of the G-acto-S1 complex, and n is the number of binding sites for S1 on actin. All parameters were obtained by nonlinear least-squares analysis using the Marquardt–Levenberg algorithm [discussed by Press et al. (1987)] implemented in the program MARQ-IT written by A. A. Kasprzak.

RESULTS

Binding of S1A2 to Mg^{2+}-G-Actin. In this study, I used only the A2 isoenzyme of S1 because in low ionic strengths it forms a complex with G-actin that does not polymerize (Chaussepied & Kasprzak, 1989a). The binding of S1A2 to Mg^{2+}-G-actin was followed by measuring the change in the anisotropy of either 1,5-IAEDANS conjugated to Cys-374 of actin or ϵATP bound at the nucleotide site of actin. Both methods produced very similar results (Figure 1), which were almost identical to the analogous titrations for Ca^{2+}-actin (Kasprzak, 1993). The interaction of both actin forms occurs with a K_d of about 0.1 μM, with an almost 1:1 stoichiometry.

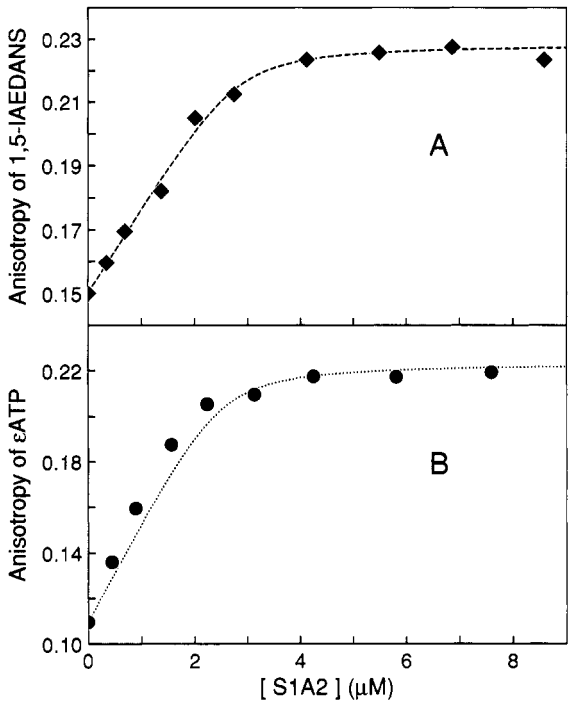

FIGURE 1: Binding isotherms of S1A2 to Mg^{2+}-G-actin obtained by measuring (A) the increase in fluorescence anisotropy of 1,5-IAEDANS-actin and (B) the increase in fluorescence anisotropy of actin-bound εATP. Samples of Mg^{2+}-actin at a concentration of 2.5 μM in buffer G_M (2 mM HEPES, 0.05 mM $MgCl_2$, 0.1 mM EGTA, 0.2 mM DTE, and 0.1 mM NaN_3, pH 7.5 at 20 °C) were prepared and mixed with S1A2 (dialyzed against 10 mM MOPS/0.4 mM DTE, pH 7), and the values of anisotropy were measured within 1–3 min. The conversion of Ca^{2+}- to Mg^{2+}-actin was made separately for each sample. The dashed lines were computed using the following values: panel A, K_d = 0.1 μM, ΔA_{max} = 0.079, and n = 1.136; panel B, K_d = 0.1 μM, ΔA_{max} = 0.114, and n = 1.

The presence of a second, albeit weak, binding site was also discernible for both types of actin although the deviations were rather small (Figure 1). I emphasize that for each of the points shown a separate $Ca^{2+} \rightarrow Mg^{2+}$-actin exchange had to be performed; serial addition of S1 to Mg^{2+}-actin produced variable results.

Absence of S1-Induced Actin Oligomers. Several laboratories reported the presence of actin oligomers in Mg^{2+}-actin preparations (Newman et al., 1985; Mozo-Villarias & Ware, 1985; Goddette et al., 1986; Attri et al., 1991). In the absence of ATP, Attri et al. (1991) found that 22% of actin at a concentration of 7.5 μM was converted to dimers in 80 min. Newman et al. (1985) also reported the formation of oligomers in 80–100 min following the addition of $MgCl_2$. Formation of nonproductive actin dimers was seen over a 4-h period following the addition of Mg^{2+} to Ca^{2+}-actin (Goddette et al., 1986). The effect of S1 on the rate or extent of oligomerization of Mg^{2+}-actin is not known; for Ca^{2+}-actin Valetin-Ranc and Carlier (1992) reported instantaneous formation of oligomeric species on addition of both isoenzymes of S1. It was, therefore, necessary to investigate this problem in detail to find out whether actin oligomers were present in the preparations used in this paper.

To ascertain reproducibility throughout this study, I always converted Ca^{2+}- to Mg^{2+}-actin for 10 min and used the product immediately. I measured the fluorescence anisotropy of 1,5-IAEDANS-labeled Ca^{2+}- and Mg^{2+}-actins at concentrations of 0.5, 1, 2, 3, 4, and 6 μM in their complexes with S1A2 at concentrations of 3.1, 3.6, 4.5, 5.5, 6.5, and 8.4 μM, respectively. The degree of actin saturation with its ligand

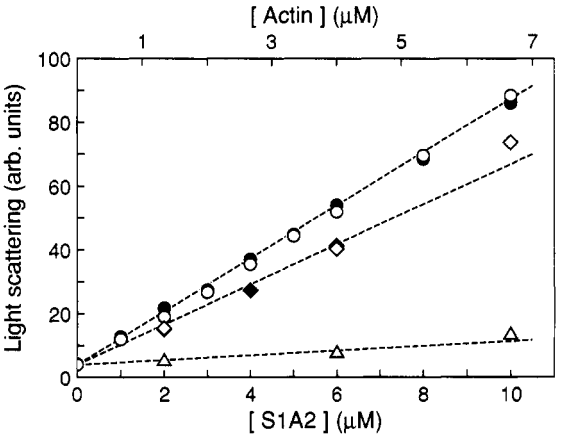

FIGURE 2: Linearity of light scattering from Ca^{2+}- and Mg^{2+}-G-acto-S1A2 complexes as a function of protein concentration. Light scattering was monitored at 400 nm: (△) Mg^{2+}-actin; (◇) S1A2 added to buffer G_M (magnesium-containing buffer); (◆) S1A2 in calcium-containing buffer; (○) Mg^{2+}-actin + S1A2; (●) Ca^{2+}-actin + S1A2.

(S1A2) was 96% in all cases. The anisotropy values were, within experimental error, identical for all samples and were equal to 0.252 ± 0.002 for Ca^{2+}-actin and 0.250 ± 0.002 for Mg^{2+}-actin. Fluorescence anisotropy has previously been known to be a sensitive tool to study changes in the aggregation state of actin. The anisotropy of either Ca^{2+}- or Mg^{2+}-1,5-IAEDANS-G-actin is 0.16; for the pPDM cross-linked dimer of actin the value of fluorescence polarization is equal to 0.29, corresponding to A = 0.215 (Chaussepied & Kasprzak, 1989b). Since the precision of anisotropy measurements is generally better than 0.005 (compare with the data described above), the presence of 10% actin *dimers* is detectable. For polymerized actin, p = 0.42 (A = 0.326) (Chaussepied & Kasprzak, 1989a). An actin oligomer consisting of four monomers is expected to have A = 0.27. In the presence of S1, the difference in anisotropy between the G-acto-S1 complex and the fully decorated filament is reduced. Nonetheless, the formation of polymeric species in the system was also easily detected (Chaussepied & Kasprzak, 1989a).

Finally, oligomers are believed to form above a certain concentration of actin. The existence of such a limiting or critical concentration was demonstrated by Attri et al. (1991) for Mg^{2+}-actin and by Valentin-Ranc and Carlier (1992) for Ca^{2+}-G-acto-S1 complexes; a value of 3.5 μM for the Ca^{2+}-G-acto-S1A2 complex was found. The phenomenon manifests itself as a sudden increase in the slope of a plot of light scattering *vs* protein concentration. I tested whether or not this occurred with the actin preparations used in this work by employing actin and S1 at concentrations of up to 7 and 10 μM, respectively; the proteins were mixed in a ratio of 1:1.5 ([actin]/[S1A2]) (Figure 2). Even when the concentrations of both proteins considerably exceeded the value of 2.5 μM, used for most experiments in this study, the plots continued to be linear, and again no difference between Ca^{2+}- and Mg^{2+}-actins was seen. I emphasize that the intensity of light scattering from these samples was exceedingly small; for a polymerized sample the intensity was more than 200-fold greater than the highest value shown in Figure 2. When S1A2 was added to samples of actin known to contain oligomers, rapid polymerization ensued (data not shown). Finally, it is noteworthy that in order to avoid excessive loss of nucleotide during the conversion of Ca^{2+}-actin to Mg^{2+}-actin, it was necessary to use the protein at a relatively high (*ca.* 20 μM) concentration. Nonetheless, the formation of oligomers is believed to be reversible as they spontaneously dissociate upon dilution (Attri et al., 1991). In

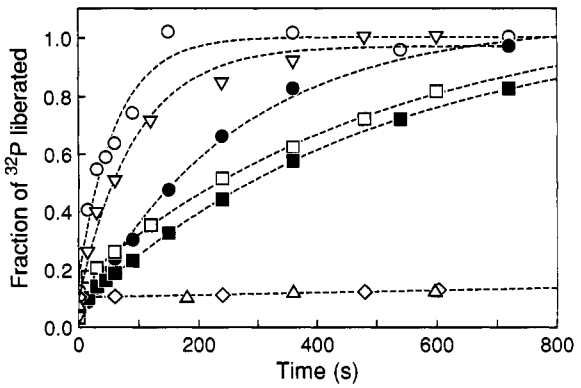

FIGURE 3: Effect of S1A2 on the time course of ^{32}P liberation from ATP-Mg^{2+}-actin: [Mg^{2+}-actin] = 2.5 μM in buffer G_M, except for (△) where Ca^{2+}-actin was used at the same concentration and in the absence of Mg^{2+} ([S1A2] = 7.8 μM (where indicated)); (○) [γ-^{32}P]-ATP-actin + S1A2 + alkaline phosphatase; (●) [α-^{32}P]ATP-actin + S1A2 + alkaline phosphatase; (□) [γ-^{32}P]ATP-actin + alkaline phosphatase; (■) [α-^{32}P]ATP-actin + alkaline phosphatase; (◇) [γ-^{32}P]ATP-actin; (△) [γ-^{32}P]ATP-Ca^{2+}-actin + S1A2 + alkaline phosphatase; (▽) [γ-^{32}P]ATP-Mg^{2+}-actin + S1A2, no alkaline phosphatase. The dashed lines were computed using the values of k_- given in Table 1.

conclusion, several complemetary sets of experiments are consistent with the idea that, in the samples used for the present study, no significant amount of oligomers was present.

Stability of the Mg^{2+}-G-Acto-S1A2 Complex during Kinetic Measurements. When the rates of nucleotide or Mg^{2+} dissociation from the G-acto-S1 complex are measured, a nucleotide- and/or metal-free actin is generated. This protein denatures with a $t_{1/2}$ of 10 min and has properties different from those of either G- or F-actin (Gershman et al., 1988; Estes et al., 1992b). Its presence could interfere with the exchange reaction by binding nonspecifically to either S1 or native actin. I measured the fluorescence anisotropy of 2.5 μM 1,5-IAEDANS-Mg^{2+}-actin during its incubation with S1 and alkaline phosphatase for 10 min. Three different nonsaturating concentrations of S1A2 were used: 0.72, 1.44, and 2.15 μM. The measured values of fluorescence anisotropy were found to be constant during the incubation time and were equal to 0.172 ± 0.006, 0.226 ± 0.003, and 0.243 ± 0.006, respectively. Thus, despite the fact that during the incubation time most of the nucleotide dissociates from actin (see below), the constant value of the anisotropy indicated that the G-acto-S1A2 complex remained stable.

Effect of S1A2 on the Rates of ATP Dissociation and Hydrolysis by Mg^{2+}-G-Actin. To measure the rate of ATP dissociation from the G-acto-S1A2 complex, the production of radioactive orthophosphate derived from actin-bound [α-^{32}P]ATP was monitored (Figure 3). The orthophosphate was cleaved from the remaining nucleoside by a large excess of alkaline phosphatase. Since neither actin nor S1 is able to liberate P_i from the α-labeled ATP, this hydrolytic reaction has to occur in solution after the nucleotide has left the actin-binding cleft. Hence, this method measures the rate of nucleotide dissociation.

In the presence of 50 μM Mg^{2+}, the effect of S1A2 on the dissociation of the actin's nucleotide is significantly different from that seen with Ca^{2+}-actin (Kasprzak, 1993). Firstly, all values of the dissociation rates for nucletides are considerably higher for Mg^{2+}-actin (Table 1) than for Ca^{2+}-actin ($\sim 10^{-4}$). Secondly, while S1A2 partially *inhibited* the dissociation of ATP from Ca^{2+}-actin, it *accelerated* its dissociation from Mg^{2+}-actin. The latter effect of S1 was unexpected; therefore, the phosphorylation state of actin's nucleotide in the complex was examined using [γ-^{32}P]ATP (Figure 3, Table 1).

Table 1: Effect of S1A2 on the Rate Constants for Dissociation of ATP, ϵATP, ϵADP, and Mg^{2+} Bound to Mg^{2+}-G-Actin[a]

protein[b]	dissociation effected by	k_- (s^{-1}) no S1	k_- (s^{-1}) +S1A2[c]
[γ-^{32}P]ATP-actin	alkaline phosphatase	0.002 ± 0.0003	0.016 ± 0.0003
[α-^{32}P]ATP-actin	alkaline phosphatase	0.002 ± 3 × 10^{-5}	0.004 ± 0.0001
[γ-^{32}P]ATP-actin + DNase I	alkaline phosphatase	4.1 × 10^{-4} ± 2 × 10^{-5}	1.4 × 10^{-3} ± 3 × 10^{-5}
[α-^{32}P]ATP-actin + DNase I	alkaline phosphatase	2.7 × 10^{-4} ± 2 × 10^{-5}	2.2 × 10^{-4} ± 2 × 10^{-5}
ϵATP-actin	alkaline phosphatase	0.0061 ± 0.0046	0.010 ● 0.0097
	EDTA[d]	0.011 ± 0.0001	0.017 ± 0.0002
ϵADP-actin	alkaline phosphatase	0.061 ± 0.0016	0.025 ± 0.0004
	EDTA	0.12 ± 0.005	0.034 ± 0.0008

[a] The dissociation rate constants k_- were measured either by following the decrease in fluorescence of ϵATP or ϵADP or by counting the ^{32}P liberated, as described under Materials and Methods. [b] Actin concentration was 2.5 μM. [c] At saturating concentration of 8.7 μM, except for ϵATP dissociation by alkaline phosphatase for which [S1A2] = 6.4 μM. [d] 0.2 mM EDTA added to G buffer containing 50 μM Mg^{2+}.

In this case, radioactive orthophosphate can be produced on actin and, in addition, by S1 or alkaline phosphatase, after dissociation of the nucleotide from the protein. If no ATP hydrolysis occurs on actin, the rates obtained with α- and γ-labeled nucleotides should be identical, since in both cases the rate-limiting step of the reaction is nucleotide dissociation from the nucleotide-binding cleft. Indeed, this was observed in the absence of S1 (Table 1). However, in the presence of a saturating concentration of S1A2, the rate of $^{32}P_i$ liberation obtained with γ-labeled nucleotide (0.016 s^{-1}) exceeded 4 times the rate of nucleotide dissociation (0.004 s^{-1}) measured with α-labeled ATP (Table 1), leading to the conclusion that most of the nucleotide was hydrolyzed prior to its departure from the binding site. One can, therefore, predict that the presence of alkaline phosphatase should have little effect on the rate of [γ-^{32}P]ATP liberation. This is confirmed experimentally (Figure 3). The S1-induced hydrolysis of actin's ATP is seen only in Mg^{2+}-actin, and it does not occur in Ca^{2+}-actin (Figure 3).

Effect of S1A2 on the Dissociation Rates of ϵATP, ϵADP, and Mg^{2+} from G-Actin. The values of the rate constants for ethenoadenosine nucleotide and metal dissociation from Mg^{2+}-actin in the presence and absence of S1, are summarized in Table 1. The values of k_- obtained in the presence of alkaline phosphatase represent the rates for nucleotide dissociation. As the removal of the tightly bound metal ion with EDTA dramatically lowers the affinity of the nucleotide, by following the time course of the EDTA-induced decrease in the fluorescence of ϵATP or ϵADP, the rate of the *metal* dissociation from actin is measured (Nowak et al., 1988). In the absence of S1, the values of k_- were found to be in good agreement with data from other laboratories. For example, k_-(ϵATP) from Mg^{2+}-actin was reported to be 0.0043 s^{-1} at pH 7.0 (Kinossian et al., 1993). In this work k_-(ϵATP) = 0.0061 s^{-1} was measured. For the dissociation of ATP from Mg^{2+}-actin, Kinossian et al. (1993) obtained k_-(ATP) = 0.0017 s^{-1}, again at pH 7.0, *vs* 0.002 s^{-1} in the present work. For Mg^{2+} dissociation from Mg^{2+}-ϵATP-actin, Nowak et al. (1988) obtained a value of 0.007 *vs* 0.011 s^{-1} reported in Table 1. Dissociation rate constants from ADP-actin are generally an order of magnitude higher than those for ATP-actin

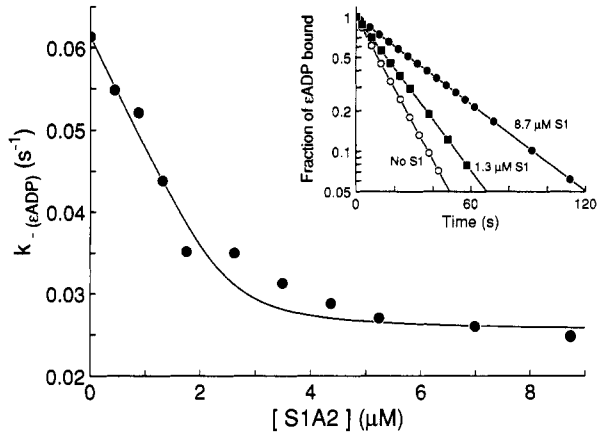

FIGURE 4: Dependence of the rate constant for dissociation of εADP from Mg^{2+}-G-actin on the concentration of S1A2 ([Mg^{2+}-εADP-actin] = 2.5 μM). The line was computed using the following binding parameters: K_d = 0.1 μM and n = 1.0. (Inset) Time course of εADP dissociation from εADP-actin for three selected concentrations of S1A2: (○) 0 μM; (■) 1.3 μM; (●) 8.7 μM. The ordinate is logarithmic.

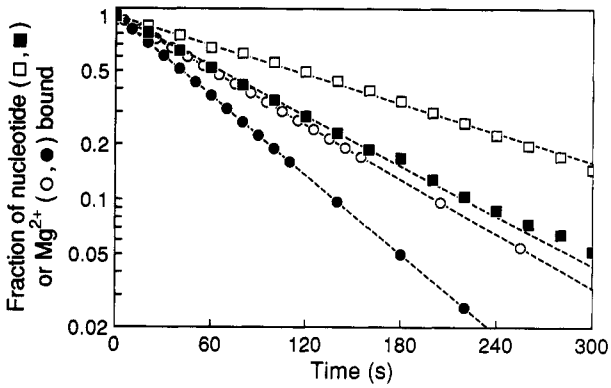

FIGURE 5: Acceleration of nucleotide and metal dissociation from εATP-Mg^{2+}-actin in the presence of S1A2 ([actin] = 2.5 μM in buffer G_M). See Materials and Methods for the amount of alkaline phosphatase used: (□) εATP-actin + alkaline phosphatase; (■) εATP-actin + S1A2 (8.75 μM) + alkaline phosphatase; (○) εATP-actin + EDTA (0.2 mM); (●) εATP-actin + S1A2 (6.4 μM) + EDTA (0.2 mM). The plot is semilogarithmic.

(Kinossian et al., 1993). As seen from Table 1, this trend also persists for ethenoadenosine nucleotides. Because of the well-known interdependence of nucleotide and metal binding to G-actin, the values of k_- for both ATP and ADP are also influenced by the Mg^{2+} concentration, often making comparisons difficult.

S1A2 inhibits the dissociation of εADP from Mg^{2+}-actin (Table 1, Figure 4). The decrease in k_- (about 2-fold) is smaller than that for Ca^{2+}-actin, where 5–8-fold inhibition was seen (Kasprzak, 1993). The reaction follows first-order kinetics rather well (Figure 4 (inset)). S1A2 had a similar effect on the rate of Mg^{2+} dissociation from εADP-actin (Table 1). Very different behavior was observed when the dissociation of either nucleotide or Mg^{2+} from the εATP-G-acto-S1A2 complex was examined (Figure 5, Table 1), in agreement with the results obtained with nonfluorescent ATP. The presence of S1 resulted in the acceleration, *ca.* 2-fold, of nucleotide and metal dissociation from actin. But this effect appears to be the consequence of ATP hydrolysis on actin, activated by S1 binding. In the G-acto-S1 complex, the dissociating nucleotide is εADP (or ADP), for which k_- is about an order of magnitude higher than that for the corresponding nucleoside triphosphate. At the same time, the presence of S1 reduces the dissociation rate constant for either ADP or ATP. However, the reduction (~2-fold) is modest and does not compensate for the much higher values of k_- for nucleotide diphosphates. These processes result in the apparent augmentation of k_-(εATP) and k_-(ATP) in the presence of S1.

The hypothesis that the acceleration of actin ATPase is a result of actin oligomerization or polymerization is implausible. First, since all ATP is hydrolyzed, the oligomerization would have to encompass the entire actin population. Considering the results of light scattering and polarization of fluorescence, described above, this seems unlikely. Second, oligomerization *per se* is insufficient to hydrolyze actin's ATP (Attri et al., 1991); only during the formation of real polymers is the hydrolytic activity of actin turned on. The amount of ATP hydrolyzed at time = 0 is shown in Figure 3; in all cases it was 5% or less.

Since the hydrolysis of ATP or εATP followed by the release of P_i and ADP (εADP) from actin consists of two sequential reactions, the concentration of the end products as a function of time may not obey first-order kinetics. However, besides the *sequential* reaction, a *parallel* reaction (direct nucleotide dissociation) is also present. A biphasic curve of nucleotide release is anticipated if the second step (the release) is slower than the first one (hydrolysis), and with the parallel reaction mentioned above, it is possible to obtain a triphasic curve under certain circumstances. Perusal of Table 1 indicates that this may occur only for ATP dissociation from the G-acto-S1A2 complex, but even in this case the effects are not expected to be dramatic since all of the rates are within 1 order of magnitude. In all other cases the rate of release is faster than the rate of hydrolysis. When the time course of nucleotide liberation from the ATP-G-acto-S1A2 complex was simulated using the values of the rate constants from Table 1, the curve (not shown) did not exhibit conspicuous multiphasic character. Moreover, the deviations from the experimental points were rather small. Also, the precision in determining the rates in the system seems insufficient to uncover deviations from simple first-order kinetics. Finally, the liberation of $^{32}P_i$ from γ-labeled ATP should not display multiphasic character, regardless of the reaction mechanism, because in this case the method follows the appearance of $^{32}P_i$, whether or not it has been released from actin.

Nucleotide Hydrolysis by Mg^{2+}-G-Actin in the Presence of DNase I and S1A2. Recently, I suggested that the inhibition of nucleotide dissociation from Ca^{2+}-G-actin by S1A2 is due to motion of the two large domains of actin (Kasprzak, 1993). DNase I binds to subdomains 2 and 4 of actin (Kabsch et al., 1990) and blocks the entrance to the nucleotide cleft as well as the motion of these domains. Since S1 can also bind to this complex with high affinity (Lheureux et al., 1993), one has a unique opportunity to examine the effect of blocking the domain motion on the S1-stimulated actin's ATPase in Mg^{2+}-actin. The results of such experiments are shown in Figure 6. Using [α-^{32}P]ATP it was found that, in the presence of DNase I, the rate of nucleotide dissociation from G-actin is dramatically reduced (Table 1), in accord with previous reports (Mannherz et al., 1980); this rate is also independent of the presence of S1A2 (Figure 6). Thus, the observed hydrolysis of [γ-^{32}P]ATP is, in this case, almost entirely due to the intrinsic ATPase activity of Mg^{2+}-G-actin. DNase I itself activates actin's ATPase [Figure 6 and Polzar et al. (1982)]. S1A2 accelerates it even more. Nonetheless, both hydrolysis rates are quite low compared to the corresponding values in the absence of DNase I.

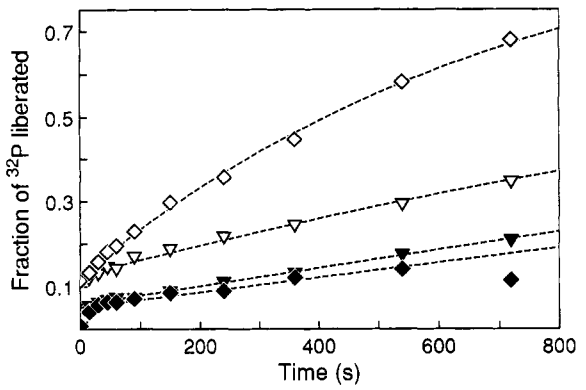

FIGURE 6: Effect of S1A2 on dissociation and hydrolysis of ATP by Mg^{2+}-actin in the presence of DNase I: [Mg^{2+}-ATP-actin] = 2.5 μM; [DNase I] = 14 μM; [S1A2] = 8.7 μM (where indicated); (◇) [γ-^{32}P]ATP-actin + S1A2 + DNase I + alkaline phosphatase; (▽) [γ-^{32}P]ATP-actin + DNase I + alkaline phosphatase; (▼) [α-^{32}P]-ATP-actin + DNase I + alkaline phosphatase; (◆) [α-^{32}P]ATP-actin + S1A2 + DNase I + alkaline phosphatase. The dashed lines were computed using the values of k_- given in Table 1.

DISCUSSION

In this work, I have presented evidence that S1A2 induces specific conformational changes in the molecule of Mg^{2+}-G-actin that lead to decreased dissociation rates of the nucleotide and of metal from the nucleotide site of actin. This behavior is quite reminiscent of the effects of S1 exerted on Ca^{2+}-G-actin (Kasprzak, 1993). However, in contrast with Ca^{2+}-actin, S1 dramatically stimulates actin's ATPase in Mg^{2+}-actin. While the interpretation of these results is rather straightforward, the structural basis for the divergent behavior of Ca^{2+}- and Mg^{2+}-actins is not. The activation of ATPase from $\sim 5 \times 10^{-5}$ to ~ 0.02 s^{-1} is one of the highest observed thus far. Brenner and Korn (1981) reported a value of 3×10^{-3} s^{-1} for cytochalasin-D activating actin's ATPase, although recently Selden et al. (1991) found a value of ~ 0.1 s^{-1} for this system under somewhat different conditions. During actin polymerization, the hydrolysis rate reaches 0.07 s^{-1} (Pollard & Weeds, 1984). Since there is virtually no information concerning the residues of actin involved in ATP hydrolysis, the following discussion must be somewhat speculative, but its conclusions are in good agreement with all available data.

S1 interaction with Mg^{2+}-G-actin results in the alteration of the spatial relation between the two domains of actin. This is consistent with the inhibition of nucleotide dissociation for both Ca^{2+}- and Mg^{2+}-actin. The new relation of the domains with respect to the ATP-binding site brings one of the groups essential for the hydrolysis (Gln-137 was suggested by Tirion and ben-Avraham (1993)) to the correct orientation, leading to the hydrolysis of the β,γ-phosphodiester bond of ATP.

On the opposite side of the nucleotide cleft, Root and Reisler (1992) proposed that Lys-213 and Lys-326 move closer to the nucleotide base when S1 binds to actin. The experiments with DNase I support the hypothesis that the domain motion is involved in hydrolysis since its presence resulted in a marked diminution of the hydrolytic activity. Such a mechanism would also bear resemblance to the well-known cases of ATP hydrolysis for hexokinase and hsc70 [see Gerstein et al. (1994) for a review]. Furthermore, it would also agree with the F-acto-S1 reconstructions (Rayment et al., 1993; Schröder et al., 1993), in which S1 interacts with the two centrally located helices of actin, particularly with helix 137–147. The interaction with the helices was proposed to mediate a scissor-type opening and closing motion of the two domains (Bork et al., 1992; Tirion & ben-Avraham, 1993). S1 binding to this somewhat hydrophobic region of the molecule is consistent with the idea that myosin head induces an F-like conformation in certain regions of the actin protomer, and this may explain the polymerization of actin by heavy meromyosin and subfragment 1. As demonstrated by Miller et al. (1988), when G-actin is present in excess over myosin head, S1 polymerizes only an equimolar amount of actin. These experiments imply that it is necessary to keep S1 bound to the actin protomer in order to induce a specific conformation of the protein that prevents the dissociation of the monomer from the filament. The closure of the nucleotide cleft, the inhibition of nucleotide dissociation, and the acceleration of ATP hydrolysis occur during actin polymerization, but perhaps to a different extent, they also occur when S1 binds to Mg^{2+}-G-actin.

Furthermore, the communication between the actomyosin interface and the nucleotide site of actin is maintained upon polymerization. The binding of heavy meromyosin not only decreased the elastic modulus of ϵADP-F-actin but changed the angles of absorption and emission dipoles of the fluorescent nucleotide (Yanagida & Oosawa, 1978). Harvey et al. (1977) observed a large, 4-ns drop in the fluorescence lifetime of ϵADP on F-actin upon binding of S1 or heavy meromyosin. More recently, Naber and Cook (1994) found that a spin-label analog of ATP on F-actin had two populations with different rotational mobilities. The binding of S1 shifted the distribution of the label toward the population with highly restricted mobility. The type of divalent metal in the actin cleft also has a significant effect on the structural changes induced by myosin head. In the presence of Ca^{2+}, the mobility of 1,5-IAEDANS attached to Cys-374 of F-actin strongly decreased upon S1 binding, in contrast to Mg^{2+}-F-actin where a cooperative increase in the mobility was seen (Miki et al., 1982).

Another aspect of this work concerns a plausible significance of the finding that actin could be a quite efficient ATPase in the regulation of cytoskeleton. Naturally, this does not involve skeletal muscle S1. However, considering the abundance of actin-binding proteins, it is likely that some of them accelerate actin's ATPase even more than S1 or at least to the same extent. Careful measurements of the effect exerted by actin-binding proteins on the rate of nucleotide hydrolysis in Mg^{2+}-actin are rare. Recently, it has been found that gelsolin not only is able to distinguish ADP-actin from the ATP monomer of actin but also activates actin's ATPase on one of the two G-actin molecules in the ternary complex (Laham et al., 1993). The stimulating effect of actin-binding proteins on the ATPase of actin may be a more widespread phenomenon than initially thought. Since about half of the ATP pool in resting platelets is hydrolyzed by actin, presumably during G- to F-actin turnover (Daniel et al., 1986), the actin ATPase is expected to be very precisely controlled. In the nucleotide-release model of the regulation of actin dynamics in cells (Theriot & Mitchison, 1992), the ratio of ADP- to ATP-actin plays a fundamental role. Recently, it has been suggested that assembly and desequestering of actin are regulated by profilin-mediated nucleotide exchange on actin and by preferential interaction of thymosin β_4 with ATP-G-actin (Goldschmidt-Clermont et al., 1992; Pantaloni & Carlier, 1993). However, this does not exclude the possibility that other mechanisms can also be involved; i.e., the pool of ADP-actin can be enriched by an actin-binding protein that stimulates the hydrolysis of actin's ATP.

ACKNOWLEDGMENT

I thank Tom Barman and Karine Lheureux for their generous gifts of γ-labeled ATP and purified DNAse I, respectively. I am indebted to Patrick Chaussepied for many helpful suggestions and criticism, and I am grateful to Ridha Kassab for support and continuing interest in this work.

REFERENCES

Attri, A. K., Lewis, M. S., & Korn, E. D. (1991) *J. Biol. Chem. 266*, 6815–6824.
Bork, P., Sander, C., & Valencia, A. (1992) *Proc. Natl. Acad. Sci. U.S.A. 89*, 7290–7294.
Brenner, S. L., & Korn, E. D. (1981) *J. Biol. Chem. 256*, 8663–8670.
Carlier, M. F., Jean, C., Rieger, K. A., Lenfant, M., & Pantaloni, D. (1993) *Proc. Natl. Acad. Sci. U.S.A. 90*, 5034–5038.
Chaussepied, P., & Kasprzak, A. A. (1989a) *Nature 342*, 950–953.
Chaussepied, P., & Kasprzak, A. A. (1989b) *J. Biol. Chem. 264*, 20752–20759.
Daniel, J. L., Molish, I. R., Robkin, L., & Holmsen, H. (1986) *Eur. J. Biochem. 156*, 677–684.
Estes, J. E., Selden, L. A., Kinosian, H. J., & Gershman, L. C. (1992a) *J. Muscle Res. Cell Motil. 13*, 272–284.
Estes, J. E., Selden, L. A., Kinosian, H. J., & Gershman, L. C. (1992b) *Biophys. J. 61*, 437a.
Gershman, L. C., Estes, J. E., & Selden, L. A. (1988) *Ann. N.Y. Acad. Sci. 529*, 264–267.
Gerstein, M., Lesk, A. M., & Chothia, C. (1994) *Biochemistry 33*, 6739–6749.
Goddette, D. W., Uberbacher, E. C., Bunick, G. J., & Frieden, C. (1986) *J. Biol. Chem. 261*, 2605–2609.
Goldschmidt-Clermont, P. J., Furman, M. I., Wachsstock D., Safer, D., Nachmias, V. T., & Pollard, T. D. (1992) *Mol. Biol. Cell 3*, 1015–1024.
Harvey, S. C., Cheung, H. C., & Thames, K. C. (1977) *Arch. Biochem. Biophys. 179*, 391–396.
Harwell, O. D., Sweeney, M. L., & Kirkpatrick, F. H. (1980) *J. Biol. Chem. 255*, 1210–1220.
Holmes, K. C., Popp, D., Gebhard, W., & Kabsch, W. (1990) *Nature 347*, 44–49.
Kabsch, W., Mannherz, H. G., Suck, D., Pai, E. F., & Holmes, K. C. (1990) *Nature 347*, 37–44.
Kasprzak, A. A. (1993) *J. Biol. Chem. 268*, 13261–13266.
Kasprzak, A. A. (1994) *Biophys. J. 66*, A195.
Kinosian, H. J., Selden, L. A., Estes, J. E., & Gershman, L. C. (1993) *J. Biol. Chem. 268*, 8683–8691.
Laham, L. E., Lamb, J. A., Allen, P. G., & Janmey, P. A. (1993) *J. Biol. Chem. 268*, 14202–14207.
Lorenz, M., Popp, D., & Holmes, K. C. (1993) *J. Mol. Biol. 234*, 826–836.
Maciver, S. K., & Weeds, A. G. (1994) *FEBS Lett. 347*, 251–256.
Mannherz, H. G., Goody, R. S., Konrad, M., & Nowak, E. (1980) *Eur. J. Biochem. 104*, 367–379.
McLaughlin, P. J., Gooch, J. T., Mannherz, H.-G., & Weeds, A. G. (1993) *Nature 364*, 685–692.
Ménétret, J.-F., Hofmann, W., Schröder, R. R., Rapp, G., & Goody, R. S. (1991) *J. Mol. Biol. 219*, 139–144.
Miki, M., Wahl, P., & Auchet, J.-C. (1982) *Biochemistry 21*, 3661–3665.
Miller, L., Kalnoski, M., Yunossi, Z., Bulinski, J. C., & Reisler, E. (1987) *Biochemistry 26*, 6064–6070.
Mozo-Villarias, A., & Ware, B. R. (1985) *Biochemistry 24*, 1544–1548.
Naber, N., & Cook, R. (1994) *Biochemistry 33*, 3855–3861.
Newman, J., Estes, J. E., Selden, L. A., & Gershman, L. C. (1985) *Biochemistry 24*, 1538–1544.
Nowak, E., Strzelecka-Golaszewska, H., & Goody, R. S. (1988) *Biochemistry 27*, 1785–1792.
Orlova, A., & Egelman, E. H. (1993) *J. Mol. Biol. 232*, 334–341.
Pantaloni, D., & Carlier, M.-F. (1993) *Cell 75*, 1007–1014.
Pollard, T. D., & Weeds, A. G. (1984) *FEBS Lett. 170*, 94–98.
Pollard, T. D., Goldberg, I., & Schwarz, W. H. (1992) *J. Biol. Chem. 267*, 20339–20345.
Press, W. H., Flannery, B. P., Teukolsky, S. A., & Vetterling, W. T. (1988) *Numerical Recipes in C. The Art of Scientific Computing*, pp 528–565, Cambrige University Press, Cambridge, U.K.
Price, P. A., Lin, L. V., Stein, W. H., & Moore, S. (1969) *J. Biol. Chem. 244*, 917–923.
Rayment, I., Holden, H., Whittaker, M., Yohn, C. B., Lorenz, M., Holmes, K. C., & Milligan, R. A. (1993) *Science 261*, 58–65.
Root, D., & Reisler, E. (1992) *Protein Sci. 1*, 1014–1022.
Schröder, R. R., Manstein, D. J., Jahn, W., Holden, H., Rayment, I., Holmes, K. C., & Spudich, J. A. (1993) *Nature 364*, 171–174.
Schutt, C. E., Myslik, J. C., Rozycki, M. D., Goonesekere, N. C., & Lindberg, U. (1993) *Nature 365*, 810–816.
Selden, L. A., Kinosian, H. J., Gershman, L. C., & Estes, J. E. (1991) *Biophys. J. 59*, 53a.
Strzelecka-Golaszewska, H., Moraczewska, J., Khaitlina, S., & Mossakowska, M. (1993) *Eur. J. Biochem. 211*, 731–742.
Theriot, J. A., & Mitchison, T. J. (1992) *Trends Cell Biol. 2*, 219–222.
Tirion, M. M., & ben-Avraham, D. (1993) *J. Mol. Biol. 230*, 186–195.
Valentin-Ranc, C., & Carlier, M.-F. (1992) *J. Biol. Chem. 267*, 21543–21550.
Valentin-Ranc, C., Combeau, C., Carlier, M. F., & Pantaloni, D. (1991) *J. Biol. Chem. 266*, 17872–17879.
Yanagida, T., & Oosawa, F. (1978) *J. Mol. Biol. 126*, 507–524.
Yanagida, T., Nakase, M., Nishiyama, K., & Oosawa, F. (1984) *Nature 307*, 58–60.